Stable high order methods for time-domain wave propagation in complex geometries and heterogeneous media

Jesse Chan

Department of Computational and Applied Mathematics, Rice University

Rice Oil and Gas HPC conference 2020

Collaborators in wave propagation

Tim Warburton (VT)

Russell Hewett (VT)

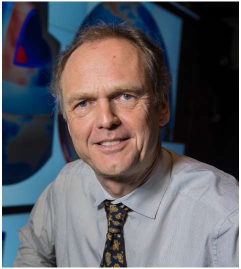

Maarten de Hoop (Rice)

Kaihang Guo (Rice, PhD 2021)

Khemraj Shukla (OK State)

Discontinuous Galerkin (DG) methods for waves

- Unstructured (tetrahedral) meshes for geometric flexibility.
- High order: low numerical dissipation and dispersion.
- High order approximations: more accurate per unknown.
- Explicit time stepping: high performance on many-core.

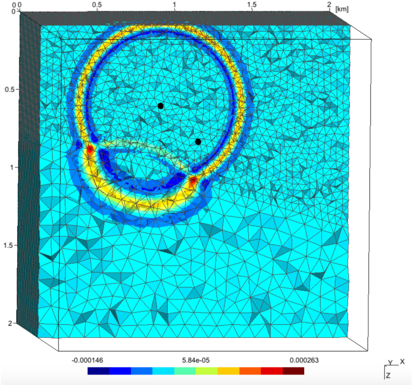

Figure courtesy of Axel Modave.

Goal: stability **and** efficiency for heterogeneous media.

Discontinuous Galerkin (DG) methods for waves

- Unstructured (tetrahedral) meshes for geometric flexibility.
- High order: low numerical dissipation and dispersion.
- High order approximations: more accurate per unknown.
- Explicit time stepping: high performance on many-core.

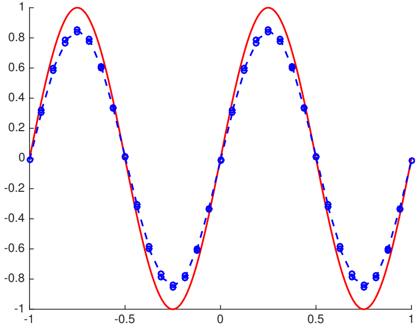

Fine linear approximation.

Goal: stability **and** efficiency for heterogeneous media.

Discontinuous Galerkin (DG) methods for waves

- Unstructured (tetrahedral) meshes for geometric flexibility.
- High order: low numerical dissipation and dispersion.
- High order approximations: more accurate per unknown.
- Explicit time stepping: high performance on many-core.

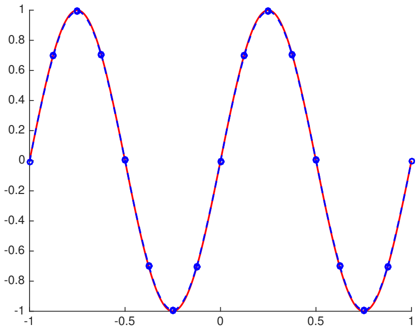

Coarse quadratic approximation.

Goal: stability **and** efficiency for heterogeneous media.

Discontinuous Galerkin (DG) methods for waves

- Unstructured (tetrahedral) meshes for geometric flexibility.
- High order: low numerical dissipation and dispersion.
- High order approximations: more accurate per unknown.
- Explicit time stepping: high performance on many-core.

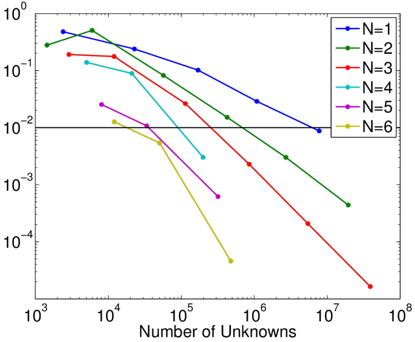

Max errors vs. dofs.

Goal: stability **and** efficiency for heterogeneous media.

Discontinuous Galerkin (DG) methods for waves

- Unstructured (tetrahedral) meshes for geometric flexibility.
- High order: low numerical dissipation and dispersion.
- High order approximations: more accurate per unknown.
- Explicit time stepping: high performance on many-core.

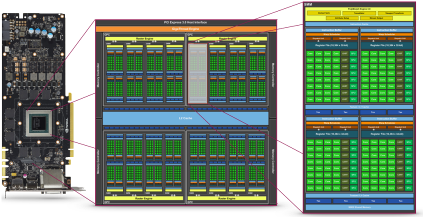

Graphics processing units (GPU).

Goal: stability **and** efficiency for heterogeneous media.

Discontinuous Galerkin (DG) methods for waves

- Unstructured (tetrahedral) meshes for geometric flexibility.
- High order: low numerical dissipation and dispersion.
- High order approximations: more accurate per unknown.
- Explicit time stepping: high performance on many-core.

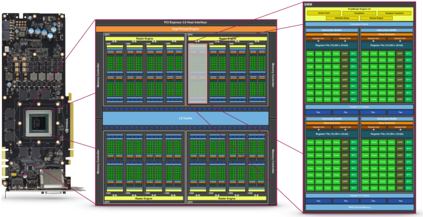

Graphics processing units (GPU).

Goal: stability **and** efficiency for heterogeneous media.

Time-domain nodal DG methods

Assume $u(\boldsymbol{x},t) = \sum \boldsymbol{u}_j \phi_j(\boldsymbol{x})$ on D^k

- Compute numerical flux at face nodes (non-local).
- Compute RHS of (local) ODE.
- Evolve (local) solution using explicit time integration (RK, AB, etc).

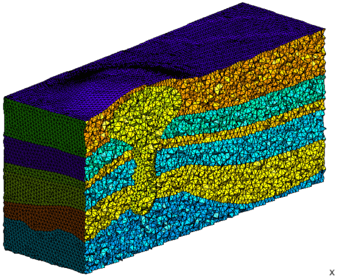

Mesh courtesy of J.F. Remacle

$$\frac{\partial u}{\partial t} = \frac{\partial u}{\partial x}$$

Example: advection equation.

$$\boldsymbol{M}_{ij} = \int_{D^k} \phi_j(\boldsymbol{x})\phi_i(\boldsymbol{x})$$

$$\mathbf{L}_f = \mathbf{M}^{-1}\mathbf{M}_f.$$

Time-domain nodal DG methods

Assume $u(\boldsymbol{x},t) = \sum \boldsymbol{u}_j \phi_j(\boldsymbol{x})$ on D^k

- Compute numerical flux at face nodes (non-local).
- Compute RHS of (local) ODE.
- Evolve (local) solution using explicit time integration (RK, AB, etc).

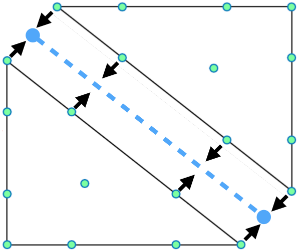

$$\frac{\mathrm{d}\mathbf{u}}{\mathrm{d}t} = \mathbf{D}_x\mathbf{u} + \sum_{\text{faces}} \mathbf{L}_f\,(\text{flux})\,.$$

$$\boldsymbol{M}_{ij} = \int_{D^k} \phi_j(\boldsymbol{x})\phi_i(\boldsymbol{x})$$

$$\mathbf{L}_f = \mathbf{M}^{-1}\mathbf{M}_f\,.$$

Time-domain nodal DG methods

Assume $u(\boldsymbol{x}, t) = \sum \boldsymbol{u}_j \phi_j(\boldsymbol{x})$ on D^k

- Compute numerical flux at face nodes (non-local).
- Compute RHS of (local) ODE.
- Evolve (local) solution using explicit time integration (RK, AB, etc).

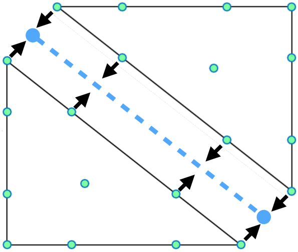

$$\frac{\mathrm{d}\mathbf{u}}{\mathrm{d}t} = \underbrace{\mathbf{D}_x \mathbf{u}}_{\text{Volume kernel}} + \underbrace{\sum_{\text{faces}} \mathbf{L}_f \left(\text{flux}\right)}_{\text{Surface kernel}}.$$

$$\boldsymbol{M}_{ij} = \int_{D^k} \phi_j(\boldsymbol{x}) \phi_i(\boldsymbol{x})$$

$$\mathbf{L}_f = \mathbf{M}^{-1} \mathbf{M}_f.$$

Time-domain nodal DG methods

Assume $u(\boldsymbol{x}, t) = \sum \boldsymbol{u}_j \phi_j(\boldsymbol{x})$ on D^k

- Compute numerical flux at face nodes (non-local).
- Compute RHS of (local) ODE.
- Evolve (local) solution using explicit time integration (RK, AB, etc).

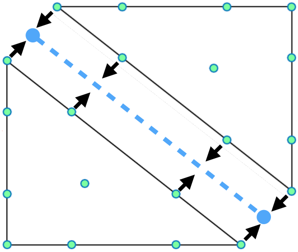

$$\underbrace{\frac{\mathrm{d}\mathbf{u}}{\mathrm{d}t}}_{\text{Update kernel}} = \underbrace{\mathbf{D}_x \mathbf{u}}_{\text{Volume kernel}} + \underbrace{\sum_{\text{faces}} \mathbf{L}_f \, (\text{flux})}_{\text{Surface kernel}}.$$

$$\boldsymbol{M}_{ij} = \int_{D^k} \phi_j(\boldsymbol{x}) \phi_i(\boldsymbol{x})$$

$$\mathbf{L}_f = \mathbf{M}^{-1} \mathbf{M}_f.$$

High order approximation of smoothly varying media

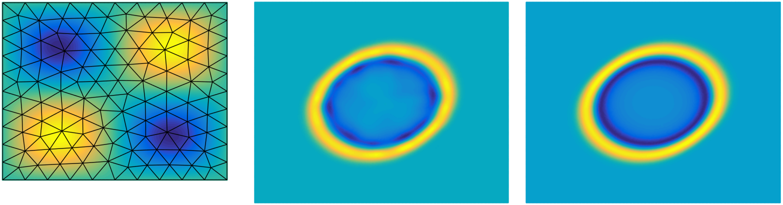

(a) Mesh and exact c^2 (b) Piecewise const. c^2 (c) High order c^2

- Piecewise const. c^2: energy stable and efficient, but inaccurate.

$$\frac{1}{c^2(\boldsymbol{x})}\frac{\partial p}{\partial t} + \nabla \cdot \boldsymbol{u} = 0, \qquad \frac{\partial \boldsymbol{u}}{\partial t} + \nabla p = 0.$$

- High order wavespeeds: weighted mass matrices. Stable, but expensive (pre-computation + storage of matrix inverses)!

$$\boldsymbol{M}_{1/c^2}\frac{\mathrm{d}\boldsymbol{p}}{\mathrm{d}t} = \boldsymbol{A}_h\boldsymbol{U}, \qquad \left(\boldsymbol{M}_{1/c^2}\right)_{ij} = \int_{D^k}\frac{1}{c^2(\boldsymbol{x})}\phi_j(\boldsymbol{x})\phi_i(\boldsymbol{x}).$$

Outline

Outline

Weight-adjusted DG (WADG)

- Weight-adjusted DG: provably energy stable approx. of $\boldsymbol{M}_{1/c^2}$

$$\boldsymbol{M}_{1/c^2}\frac{\mathrm{d}\boldsymbol{p}}{\mathrm{d}t} \approx \boldsymbol{M}\left(\boldsymbol{M}_{c^2}\right)^{-1}\boldsymbol{M}\frac{\mathrm{d}\boldsymbol{p}}{\mathrm{d}t} = \boldsymbol{A}_h\boldsymbol{U}.$$

- New evaluation reuses implementation for constant wavespeed

$$\frac{\mathrm{d}\boldsymbol{p}}{\mathrm{d}t} = \underbrace{\boldsymbol{M}^{-1}\left(\boldsymbol{M}_{c^2}\right)}_{\text{modified update}} \qquad \underbrace{\boldsymbol{M}^{-1}\boldsymbol{A}_h\boldsymbol{U}}_{\text{constant wavespeed RHS}}$$

- Low-storage: form $\boldsymbol{M}_{c^2}$ on-the-fly using quadrature.

Chan, Hewett, Warburton (2017). Weight-adjusted DG methods: wave propagation in heterogeneous media.

Highlights of WADG theory

- WADG norm has same equivalence constants (doesn't hurt CFL)

$$w_{\min} \boldsymbol{u}^T \boldsymbol{M} \boldsymbol{u} \leq \boldsymbol{u}^T \boldsymbol{M}_w \boldsymbol{u} \leq w_{\max} \boldsymbol{u}^T \boldsymbol{M} \boldsymbol{u}$$

- High order accurate approx. to full inverse weighted mass matrix, local conservation if weight $w(\boldsymbol{x})$ approximated using polynomials.

- Best L^2 approximation error is $O(h^{N+1})$, while difference between full inverse weighted mass matrix and WADG is $O\left(h^{N+2}\right)$

$$\left\| P_w u - \widetilde{P}_w u \right\|_{L^2} \leq C_{w,N} h^{N+2} \left\| w \right\|_{W^{N+1,\infty}} \left\| u \right\|_{W^{N+1,2}}$$

Chan, Hewett, Warburton (2017). Weight-adjusted DG methods: wave propagation in heterogeneous media.

Highlights of WADG theory

- WADG norm has same equivalence constants (doesn't hurt CFL)

$$w_{\min} \boldsymbol{u}^T \boldsymbol{M} \boldsymbol{u} \leq \boldsymbol{u}^T \boldsymbol{M} \boldsymbol{M}_{1/w}^{-1} \boldsymbol{M} \boldsymbol{u} \leq w_{\max} \boldsymbol{u}^T \boldsymbol{M} \boldsymbol{u}$$

- High order accurate approx. to full inverse weighted mass matrix, local conservation if weight $w(\boldsymbol{x})$ approximated using polynomials.

- Best L^2 approximation error is $O(h^{N+1})$, while difference between full inverse weighted mass matrix and WADG is $O\left(h^{N+2}\right)$

$$\left\| P_w u - \widetilde{P}_w u \right\|_{L^2} \leq C_{w,N} h^{N+2} \left\| w \right\|_{W^{N+1,\infty}} \left\| u \right\|_{W^{N+1,2}}$$

Chan, Hewett, Warburton (2017). Weight-adjusted DG methods: wave propagation in heterogeneous media.

WADG: nearly identical to DG w/weighted mass matrices

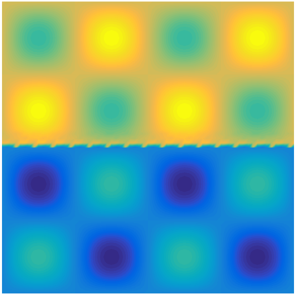

(a) $c^2(x, y)$

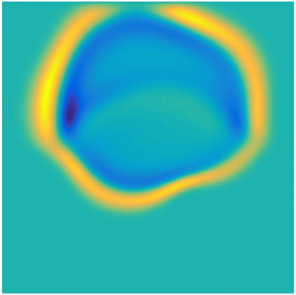

(b) Standard DG

Figure: Standard vs. weight-adjusted DG with spatially varying c^2.

- The L^2 error is $O(h^{N+1})$, but the difference between the DG and WADG solutions is $O(h^{N+2})$!

WADG: nearly identical to DG w/weighted mass matrices

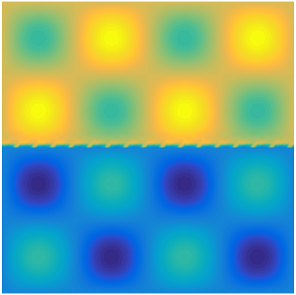

(a) $c^2(x,y)$

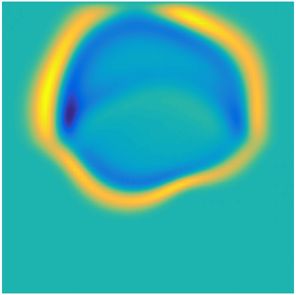

(b) Weighted-adjusted DG

Figure: Standard vs. weight-adjusted DG with spatially varying c^2.

- The L^2 error is $O(h^{N+1})$, but the difference between the DG and WADG solutions is $O(h^{N+2})$!

WADG: more efficient than storing $\boldsymbol{M}_{1/c^2}^{-1}$ on GPUs

	$N=1$	$N=2$	$N=3$	$N=4$	$N=5$	$N=6$	$N=7$
$\boldsymbol{M}_{1/c^2}^{-1}$	.66	2.79	9.90	29.4	73.9	170.5	329.4
WADG	0.59	1.44	4.30	13.9	43.0	107.8	227.7
Speedup	1.11	1.94	2.30	2.16	1.72	1.58	1.45

Time (ns) per element: storing/applying $\boldsymbol{M}_{1/c^2}^{-1}$ vs WADG (deg. $2N$ quadrature).

- Low storage matrix-free application of $\boldsymbol{M}^{-1}\boldsymbol{M}_{c^2}$ using **quadrature**-based interpolation and L^2 projection matrices $\boldsymbol{V}_q, \boldsymbol{P}_q$.

$$(\boldsymbol{M})^{-1}\boldsymbol{M}_{c^2} = \underbrace{\boldsymbol{M}^{-1}\boldsymbol{V}_q^T\boldsymbol{W}}_{\boldsymbol{P}_q}\operatorname{diag}\left(c^2\right)\boldsymbol{V}_q.$$

WADG: more efficient than storing M_{1/c^2}^{-1} on GPUs

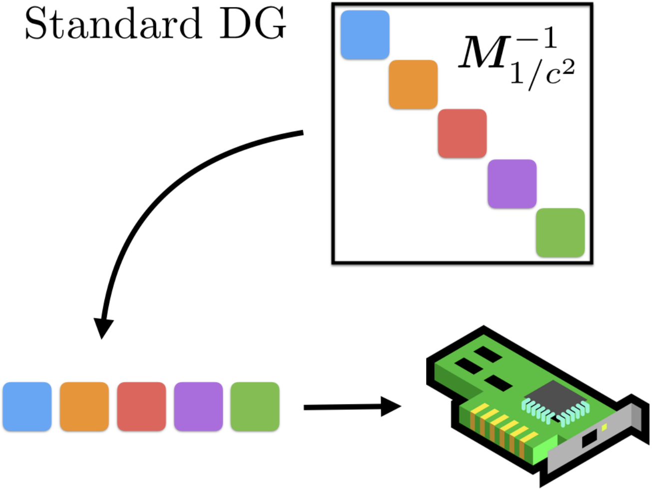

Efficiency on GPUs: reduce memory accesses and data movement!

WADG: more efficient than storing M^{-1}_{1/c^2} on GPUs

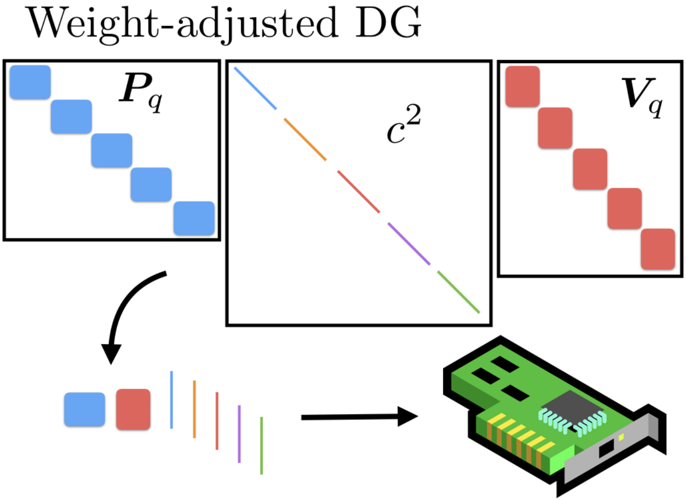

Efficiency on GPUs: reduce memory accesses and data movement!

Outline

Matrix-valued weights and elastic wave propagation

- Symmetric velocity-stress formulation (entries of $\boldsymbol{A}_i$ are ± 1 or 0)

$$\rho \frac{\partial \boldsymbol{v}}{\partial t} = \sum_{i=1}^{d} \boldsymbol{A}_i^T \frac{\partial \boldsymbol{\sigma}}{\partial \boldsymbol{x}_i}, \qquad \boldsymbol{C}^{-1} \frac{\partial \boldsymbol{\sigma}}{\partial t} = \sum_{i=1}^{d} \boldsymbol{A}_i \frac{\partial \boldsymbol{v}}{\partial \boldsymbol{x}_i}.$$

- DG formulation: *simple* penalty fluxes, matrix-weighted mass matrix

$$\boldsymbol{A}_1^T = \begin{pmatrix} 1 & 0 & 0 & 0 & 0 & 0 \\ 0 & 0 & 0 & 0 & 0 & 1 \\ 0 & 0 & 0 & 0 & 1 & 0 \end{pmatrix}, \qquad \boldsymbol{M}_{\boldsymbol{C}^{-1}} = \begin{pmatrix} \boldsymbol{M}_{C_{11}^{-1}} & \dots & \boldsymbol{M}_{C_{1d}^{-1}} \\ \vdots & \ddots & \vdots \\ \boldsymbol{M}_{C_{d1}^{-1}} & \dots & \boldsymbol{M}_{C_{dd}^{-1}} \end{pmatrix}$$

- Weight-adjusted approx. to $(\boldsymbol{M}_{\boldsymbol{C}^{-1}})^{-1}$ decouples each component

$$\boldsymbol{M}_{\boldsymbol{C}^{-1}}^{-1} \approx \left(\boldsymbol{I} \otimes \boldsymbol{M}^{-1}\right) \boldsymbol{M}_{\boldsymbol{C}} \left(\boldsymbol{I} \otimes \boldsymbol{M}^{-1}\right).$$

Simple to incorporate anisotropic media

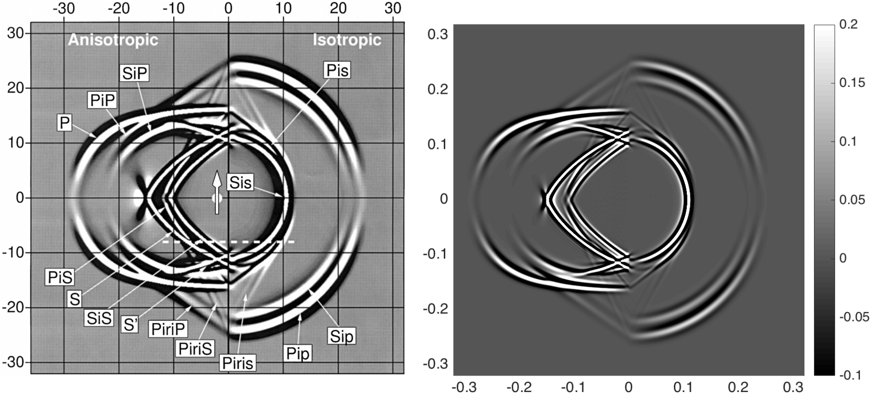

(a) Reference solution (b) WADG solution

Figure: Anisotropic media simply involves modifying the definition of $\boldsymbol{C}$.

Komatitsch, Barnes, Tromp (2000). *Simulation of anisotropic wave propagation based upon a spectral element method.*

Chan (2018). Weight-adjusted DG methods: matrix-valued weights and elastic wave prop. in heterogeneous media.

Energy stable acoustic-elastic coupling (with Guo)

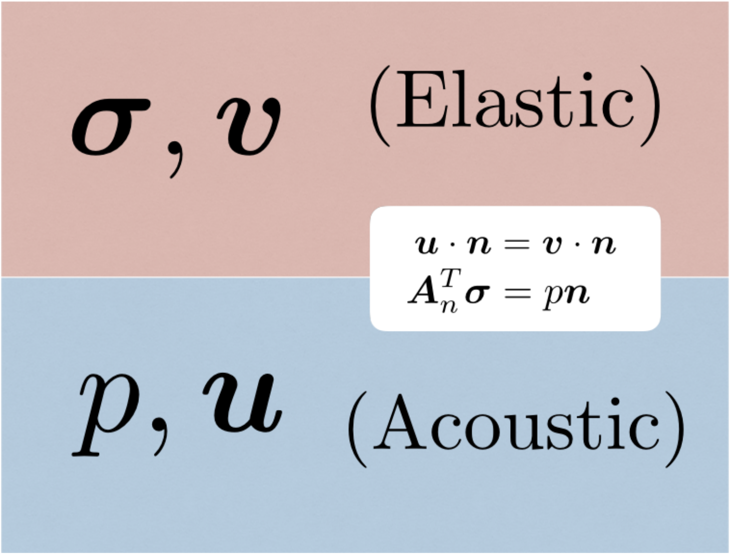

Energy stable acoustic-elastic coupling (with Guo)

$$\boxed{(\mathfrak{F}\boldsymbol{q})^* = \mathfrak{F}^-\boldsymbol{q}^- + \frac{\boldsymbol{n}\cdot[\![\boldsymbol{S}]\!] + \rho^+ c_p^+ [\![\boldsymbol{v}]\!]}{\rho^+ c_p^+ + \rho^- c_p^-}\begin{pmatrix}\boldsymbol{n}\otimes\boldsymbol{n}\\ \rho^- c_p^- \boldsymbol{n}\end{pmatrix}.}$$

$$\begin{aligned}(\mathfrak{F}\boldsymbol{q})^* &= \mathfrak{F}^-\boldsymbol{q}^- + \frac{c_p^- c_p^+ \boldsymbol{n}\cdot[\![\boldsymbol{S}]\!] + c_p^-(\lambda^+ + 2\mu^+)[\![\boldsymbol{v}]\!]}{c_p^+(\lambda^- + 2\mu^-) + c_p^-(\lambda^+ + 2\mu^+)}\begin{pmatrix}\boldsymbol{n}\otimes\boldsymbol{n}\\ \rho^- c_p^- \boldsymbol{n}\end{pmatrix} + \left(\frac{c_s^- c_s^+}{\mu^+ c_s^- + \mu^- c_s^+}\boldsymbol{s}\cdot[\![\boldsymbol{S}]\!] + \frac{c_s^- \mu^+}{\mu^+ c_s^- + \mu^- c_s^+}\boldsymbol{s}\cdot[\boldsymbol{v}]\right)\begin{pmatrix}\mathrm{sym}(\boldsymbol{s}\otimes\boldsymbol{n})\\ \rho^- c_s^- \boldsymbol{s}\end{pmatrix}\\
&+ \left(\frac{c_s^- c_s^+}{\mu^+ c_s^- + \mu^- c_s^+}\boldsymbol{t}\cdot[\![\boldsymbol{S}]\!] + \frac{c_s^- \mu^+}{\mu^+ c_s^- + \mu^- c_s^+}\boldsymbol{t}\cdot[\boldsymbol{v}]\right)\begin{pmatrix}\mathrm{sym}(\boldsymbol{t}\otimes\boldsymbol{n})\\ \rho^- c_s^- \boldsymbol{t}\end{pmatrix} = \mathfrak{F}^-\boldsymbol{q}^- + \frac{c_p^- c_p^+ \boldsymbol{n}\cdot[\![\boldsymbol{S}]\!] + c_p^-(\lambda^+ + 2\mu^+)[\![\boldsymbol{v}]\!]}{c_p^+(\lambda^- + 2\mu^-) + c_p^-(\lambda^+ + 2\mu^+)}\begin{pmatrix}\boldsymbol{n}\otimes\boldsymbol{n}\\ \rho^- c_p^- \boldsymbol{n}\end{pmatrix}\\
&- \frac{c_s^- c_s^+}{\mu^+ c_s^- + \mu^- c_s^+}\begin{pmatrix}\mathrm{sym}(\boldsymbol{n}\otimes(\boldsymbol{n}\times(\boldsymbol{n}\times[\![\boldsymbol{S}]\!])))\\ \rho^- c_s^- \boldsymbol{n}\times(\boldsymbol{n}\times[\![\boldsymbol{S}]\!])\end{pmatrix} - \frac{c_s^- \mu^+}{\mu^+ c_s^- + \mu^- c_s^+}\begin{pmatrix}\mathrm{sym}(\boldsymbol{n}\otimes(\boldsymbol{n}\times(\boldsymbol{n}\times[\boldsymbol{v}])))\\ \rho^- c_s^- \boldsymbol{n}\times(\boldsymbol{n}\times[\boldsymbol{v}])\end{pmatrix},\end{aligned}$$

$$\boxed{(\mathfrak{F}\boldsymbol{q})^* = \mathfrak{F}^-\boldsymbol{q}^- + \frac{\boldsymbol{n}\cdot[\![\boldsymbol{S}]\!] + \rho^+ c_p^+ [\![\boldsymbol{v}]\!]}{\rho^+ c_p^+ + \rho^- c_p^-}\begin{pmatrix}\boldsymbol{n}\otimes\boldsymbol{n}\\ \rho^- c_p^- \boldsymbol{n}\end{pmatrix} - \frac{1}{\rho^- c_s^-}\begin{pmatrix}\mathrm{sym}(\boldsymbol{n}\otimes(\boldsymbol{n}\times(\boldsymbol{n}\times[\![\boldsymbol{S}]\!])))\\ \rho^- c_s^- \boldsymbol{n}\times(\boldsymbol{n}\times[\![\boldsymbol{S}]\!])\end{pmatrix}.}$$

- Traditional upwind acoustic-elastic fluxes are complex to derive.
- Cannot prove energy stability in the case of heterogeneous media.

Wilcox, Stadler, Burstedde, Ghattas (2010). *A high-order discontinuous Galerkin method for wave propagation through coupled elastic–acoustic media*.

Energy stable acoustic-elastic coupling (with Guo)

$$\boldsymbol{A}_n = \boldsymbol{A}_1 n_x + \boldsymbol{A}_2 n_y + \boldsymbol{A}_3 n_z$$

(Elastic)

$$\frac{1}{2}\left(\boldsymbol{A}_n^T(\boldsymbol{\sigma}^+ - \boldsymbol{\sigma}) + \tau_{\boldsymbol{v}} \boldsymbol{A}_n^T \boldsymbol{A}_n(\boldsymbol{v}^+ - \boldsymbol{v})\right)$$

$$\frac{1}{2}\left(\boldsymbol{A}_n(\boldsymbol{v}^+ - \boldsymbol{v}) + \tau_{\boldsymbol{\sigma}} \boldsymbol{A}_n \boldsymbol{A}_n^T(\boldsymbol{\sigma}^+ - \boldsymbol{\sigma}) \cdot \boldsymbol{n}\right) \boldsymbol{n}$$

$$\frac{1}{2}\left((\boldsymbol{u}^+ - \boldsymbol{u}) \cdot \boldsymbol{n} + \tau_p (p^+ - p)\right)$$

$$\frac{1}{2}\left((p^+ - p) + \tau_{\boldsymbol{u}} (\boldsymbol{u}^+ - \boldsymbol{u}) \cdot \boldsymbol{n}\right) \boldsymbol{n}$$

(Acoustic)

Energy stable acoustic-elastic coupling (with Guo)

(Elastic)

$$\frac{1}{2}\boldsymbol{A}_n\left(\boldsymbol{n}\boldsymbol{n}^T(\boldsymbol{u}-\boldsymbol{v})+\tau_{\boldsymbol{\sigma}}\left(p\boldsymbol{n}-\boldsymbol{A}_n^T\boldsymbol{\sigma}\right)\right)$$

$$\frac{1}{2}\boldsymbol{n}^T\left(p\boldsymbol{n}-\boldsymbol{A}_n^T\boldsymbol{\sigma}+\left(\boldsymbol{I}-\boldsymbol{n}\boldsymbol{n}^T\right)\boldsymbol{A}_n^T\boldsymbol{\sigma}+\tau_{\boldsymbol{v}}(\boldsymbol{u}-\boldsymbol{v})\right)$$

$$\boldsymbol{u}\cdot\boldsymbol{n}=\boldsymbol{v}\cdot\boldsymbol{n}$$
$$\boldsymbol{A}_n^T\boldsymbol{\sigma}=p\boldsymbol{n}$$

$$\frac{1}{2}\boldsymbol{n}^T\left(\boldsymbol{v}-\boldsymbol{u}+\tau_p\left(\boldsymbol{A}_n^T\boldsymbol{\sigma}-p\boldsymbol{n}\right)\right)$$

$$\frac{1}{2}\boldsymbol{n}\boldsymbol{n}^T\left(\boldsymbol{A}_n^T\boldsymbol{\sigma}-p\boldsymbol{n}+\tau_{\boldsymbol{u}}(\boldsymbol{v}-\boldsymbol{u})\right)$$

(Acoustic)

Numerical results: coupled acoustic-elastic media

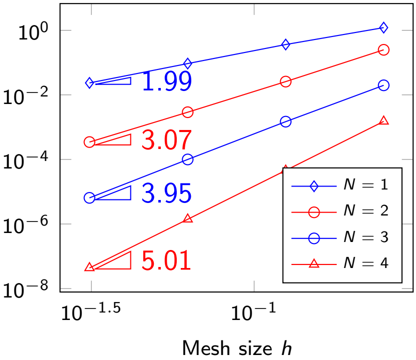

(a) Snell's law solution

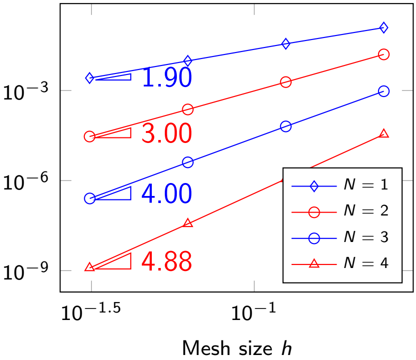

(b) Scholte wave solution

High order convergence of L^2 error for acoustic-elastic media.

Example with isotropic-anisotropic acoustic-elastic media

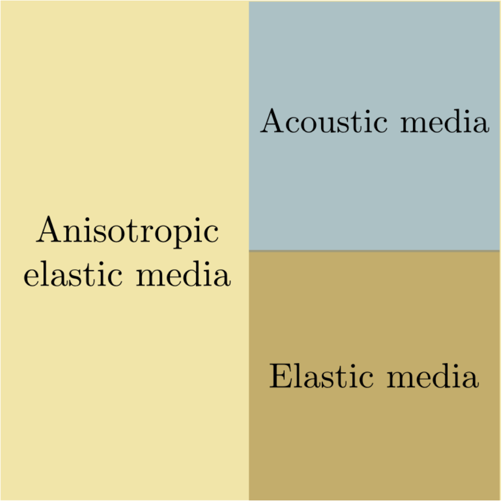

Komatitsch, Barnes, Tromp (2000). *Simulation of anisotropic wave propagation based upon a spectral element method.*

Guo, Acosta, Chan (2019). A weight-adjusted DG method for wave propagation in coupled elastic-acoustic media.

Example with isotropic-anisotropic acoustic-elastic media

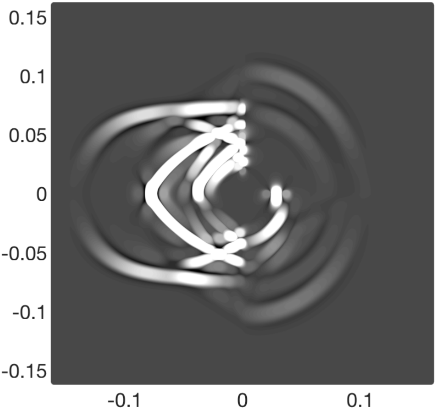

(a) $T = 30\mu s$

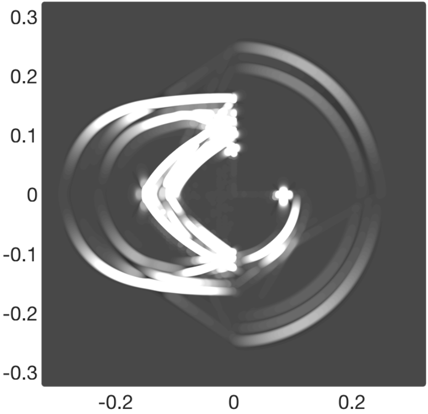

(b) $T = 60\mu s$

Piecewise constant anisotropic-isotropic acoustic-elastic media.

Komatitsch, Barnes, Tromp (2000). *Simulation of anisotropic wave propagation based upon a spectral element method.*

Guo, Acosta, Chan (2019). A weight-adjusted DG method for wave propagation in coupled elastic-acoustic media.

Example with isotropic-anisotropic acoustic-elastic media

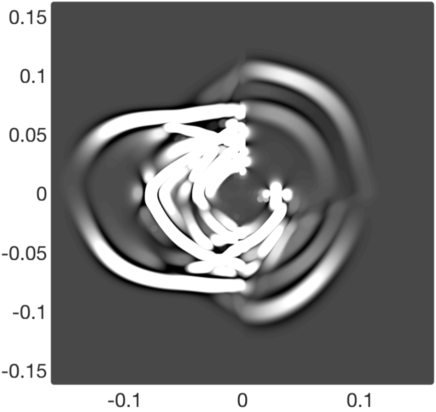

(a) $T = 30\mu s$

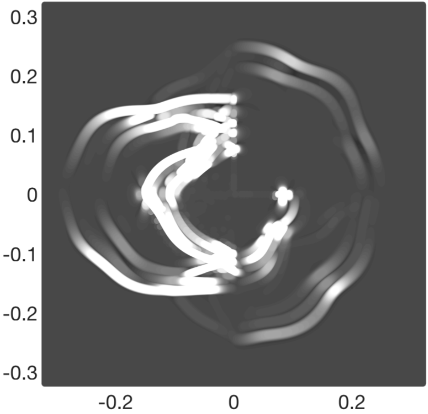

(b) $T = 60\mu s$

Piecewise smoothly varying anisotropic-isotropic acoustic-elastic media.

Komatitsch, Barnes, Tromp (2000). *Simulation of anisotropic wave propagation based upon a spectral element method.*

Guo, Acosta, Chan (2019). A weight-adjusted DG method for wave propagation in coupled elastic-acoustic media.

Outline

Computational costs at high orders of approximation

Problem: WADG at high orders becomes **expensive**!

WADG runtimes

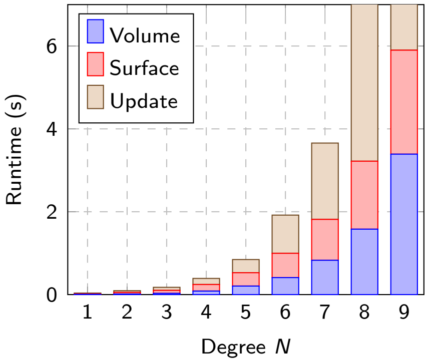

- Large **dense** matrices: $O(N^6)$ work per element.
- Idea: choose basis such that matrices are **sparse**.

WADG runtimes for 50 timesteps, 98304 elements.

BBDG: Bernstein-Bezier DG methods

- Nodal DG: $O(N^6)$ cost in 3D vs $O(N^3)$ degrees of freedom.
- Switch to Bernstein basis: sparse and structured matrices.
- Optimal $O(N^3)$ application of differentiation and lifting matrices.

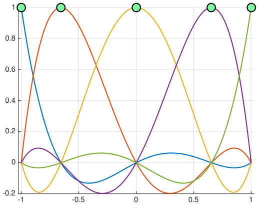

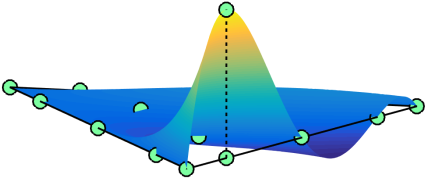

Nodal bases in one, two, and three dimensions.

Chan, Warburton 2017. GPU-accelerated Bernstein-Bezier discontinuous Galerkin methods for wave propagation (SISC).

BBDG: Bernstein-Bezier DG methods

- Nodal DG: $O(N^6)$ cost in 3D vs $O(N^3)$ degrees of freedom.
- Switch to Bernstein basis: sparse and structured matrices.
- Optimal $O(N^3)$ application of differentiation and lifting matrices.

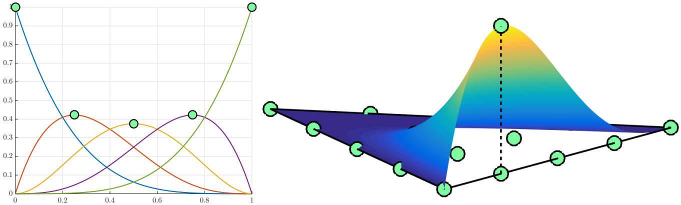

Bernstein bases in one, two, and three dimensions.

Chan, Warburton 2017. GPU-accelerated Bernstein-Bezier discontinuous Galerkin methods for wave propagation (SISC).

BBDG: Bernstein-Bezier DG methods

- Nodal DG: $O(N^6)$ cost in 3D vs $O(N^3)$ degrees of freedom.
- Switch to Bernstein basis: sparse and structured matrices.
- Optimal $O(N^3)$ application of differentiation and lifting matrices.

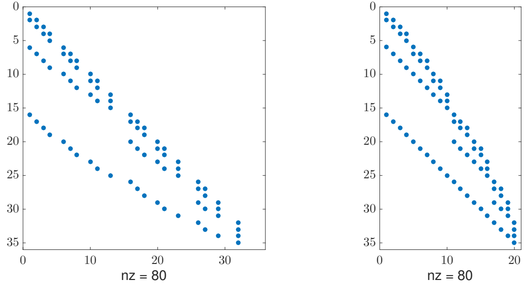

Tetrahedral Bernstein differentiation and degree elevation matrices.

Chan, Warburton 2017. GPU-accelerated Bernstein-Bezier discontinuous Galerkin methods for wave propagation (SISC).

BBDG: Bernstein-Bezier DG methods

- Nodal DG: $O(N^6)$ cost in 3D vs $O(N^3)$ degrees of freedom.
- Switch to Bernstein basis: sparse and structured matrices.
- Optimal $O(N^3)$ application of differentiation and lifting matrices.

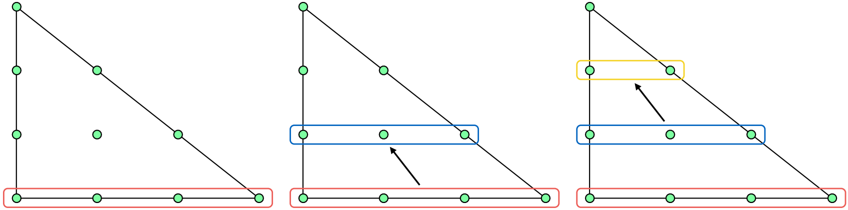

Optimal $O(N^3)$ complexity "slice-by-slice" application of Bernstein lift.

Chan, Warburton 2017. GPU-accelerated Bernstein-Bezier discontinuous Galerkin methods for wave propagation (SISC).

BBDG: efficient volume, surface kernels

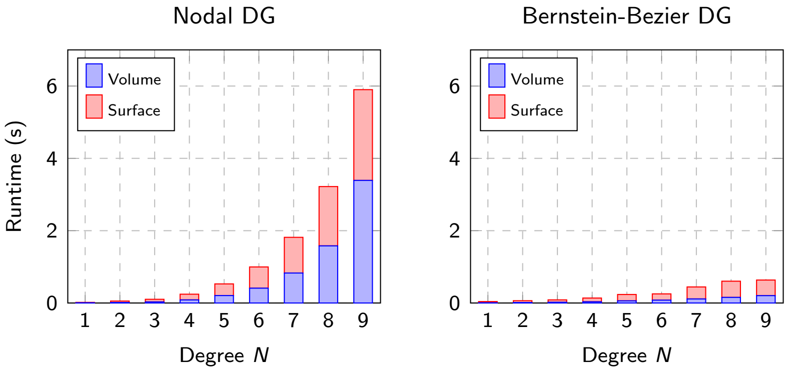

$$\underbrace{\frac{\mathrm{d}\mathbf{u}}{\mathrm{d}t}}_{\text{Update kernel}} = \underbrace{\mathbf{D}_x\mathbf{u}}_{\text{Volume kernel}} + \underbrace{\sum_{\text{faces}} \mathbf{L}_f\,(\text{flux})}_{\text{Surface kernel}}, \qquad \mathbf{L}_f = \mathbf{M}^{-1}\mathbf{M}_f.$$

A faster BBWADG update kernel (with Guo)

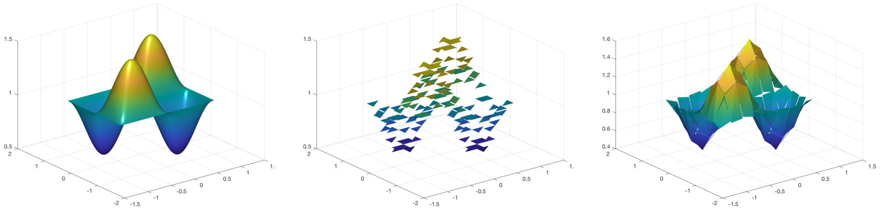

(a) Exact c^2 (b) $M = 0$ approximation (c) $M = 1$ approximation

- Exploit continuous WADG steps: given $u(\boldsymbol{x})$, compute

$$P_N\left(u(\boldsymbol{x})c^2(\boldsymbol{x})\right), \qquad P_N = L^2 \text{ projection operator.}$$

- Our approach: approx. $c^2(\boldsymbol{x})$ with degree M polynomial, use fast Bernstein algorithms for polynomial multiplication and projection.
- Can reuse fast $O(N^3)$ Bernstein-based volume and surface kernels.

BBWADG: effect of approximating c^2 on accuracy

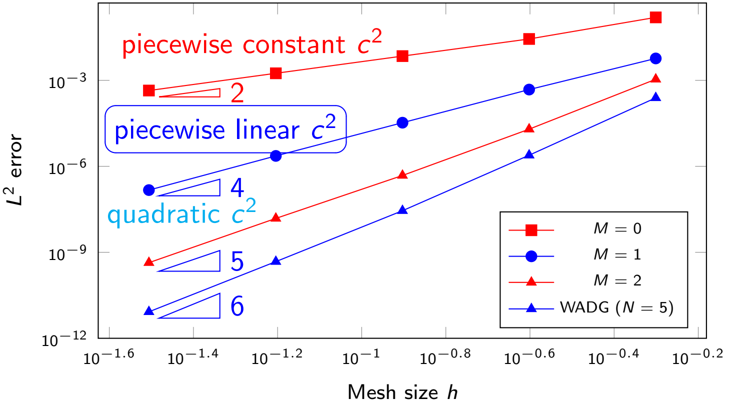

Approximating smooth $c^2(\boldsymbol{x})$ using L^2 projection:
$O(h^2)$ for $M = 0$, $O(h^4)$ for $M = 1$, $O(h^{M+3})$ for $0 < M \leq N - 2$.

Fast Bernstein polynomial multiplication

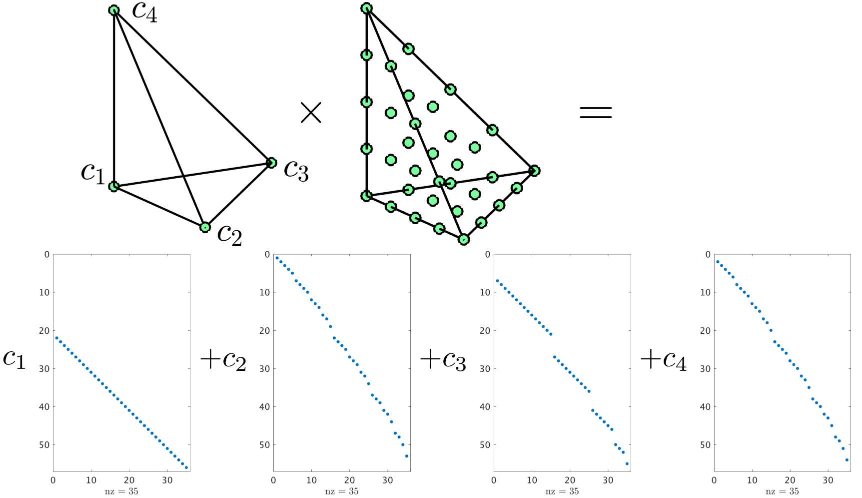

Bernstein polynomial multiplication ($M = 1$ shown), $O(N^3)$ cost for fixed M.

Fast Bernstein polynomial projection

- Given $c^2(\boldsymbol{x})u(\boldsymbol{x})$ as a degree $(N+M)$ polynomial, apply L^2 projection matrix $\boldsymbol{P}_N^{N+M}$ to reduce to degree N.
- Polynomial L^2 projection matrix $\boldsymbol{P}_N^{N+M}$ under Bernstein basis:

$$\boldsymbol{P}_N^{N+M} = \underbrace{\sum_{j=0}^{N} c_j \boldsymbol{E}_{N-j}^{N} \left(\boldsymbol{E}_{N-j}^{N}\right)^T}_{\tilde{\boldsymbol{P}}_N} \left(\boldsymbol{E}_N^{N+M}\right)^T$$

- "Telescoping" form of $\tilde{\boldsymbol{P}}_N$: $O(N^4)$ complexity, more GPU-friendly.

$$\left(c_0 \boldsymbol{I} + \boldsymbol{E}_{N-1}^{N} \left(c_1 \boldsymbol{I} + \boldsymbol{E}_{N-2}^{N-1} \left(c_2 \boldsymbol{I} + \cdots\right) \left(\boldsymbol{E}_{N-2}^{N-1}\right)^T\right) \left(\boldsymbol{E}_{N-1}^{N}\right)^T\right)$$

Sketch of GPU algorithm for $\tilde{P}_N$

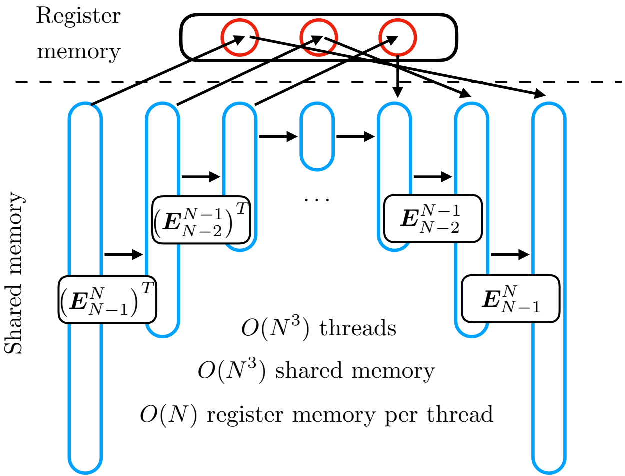

$$\left(c_0 \boldsymbol{I} + \boldsymbol{E}^N_{N-1}\left(c_1 \boldsymbol{I} + \boldsymbol{E}^{N-1}_{N-2}\left(c_2 \boldsymbol{I} + \cdots\right)\left(\boldsymbol{E}^{N-1}_{N-2}\right)^T\right)\left(\boldsymbol{E}^N_{N-1}\right)^T\right)$$

BBWADG: computational runtime (3D acoustics)

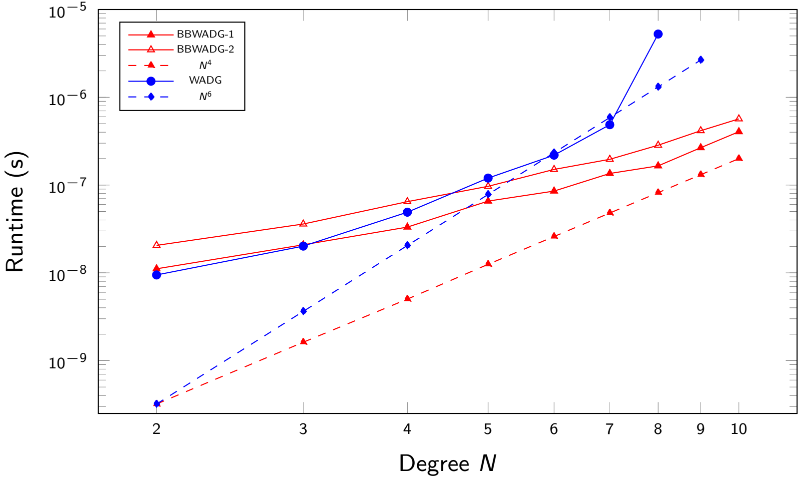

Per-element runtimes of update kernels for BBWADG vs WADG (acoustic). We observe an asymptotic complexity of $O(N^4)$ per element for $N \gg 1$.

Outline

Poro-elastic media (with V. de Hoop and Shukla)

(a) Orthotropic sandstone

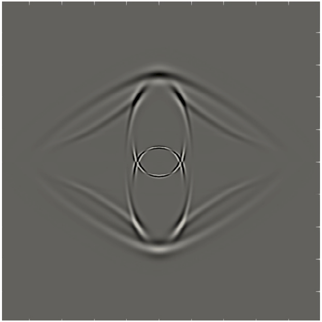

(b) Epoxy glass

- 3 wave-speed system derived from generalized dynamic Darcy's law by assuming different velocities for solid and fluid particles.
- In 3D: 7 stress components (6 stress tensor variables + scalar fluid pressure) and 6 velocity components.

High order DG vs WADG for poro-elasticity

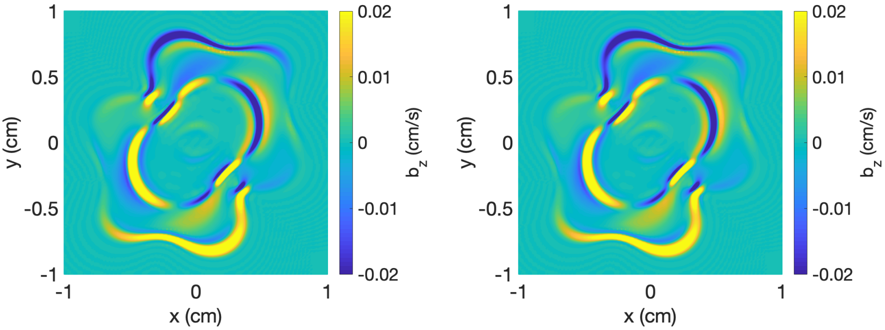

(a) DG (piecewise constant media)

(b) WADG (high order media)

Degree $N = 2$ polynomials, 64×64 uniform mesh.

WADG is again provably stable and high order accurate.

High order DG vs WADG for poro-elasticity

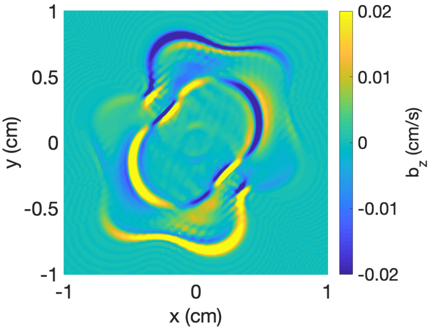

(a) DG (piecewise constant media)

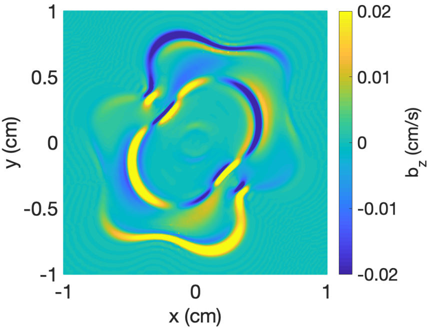

(b) WADG (high order media)

Degree $N = 4$ polynomials, 32×32 uniform mesh.

WADG is again provably stable and high order accurate.

High order DG vs WADG for poro-elasticity

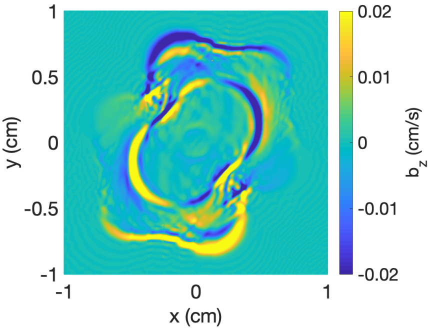

(a) DG (piecewise constant media)

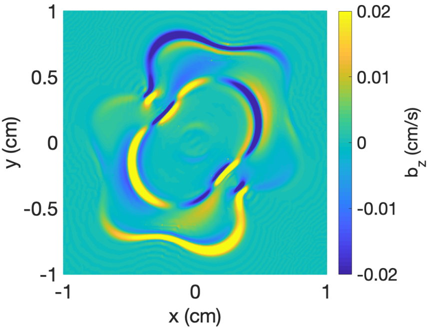

(b) WADG (high order media)

Degree $N = 8$ polynomials, 16×16 uniform mesh.

WADG is again provably stable and high order accurate.

Comparison of high order SPECFEM and WADG for a poro-elastic heterogeneous medium

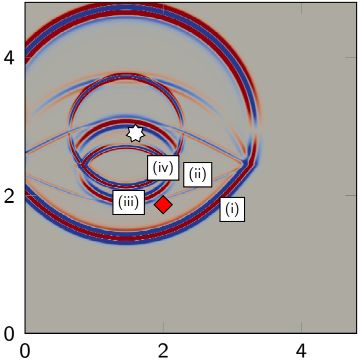

(a) Vertical solid particle velocity

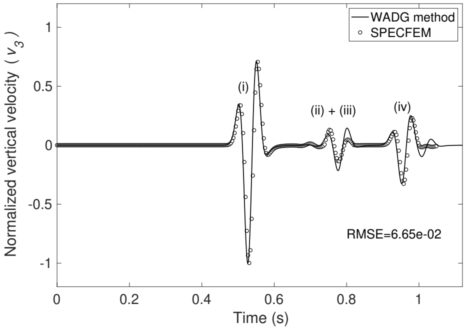

(b) Trace showing fast/slow P and S waves

A model poro-elastic reservoir problem

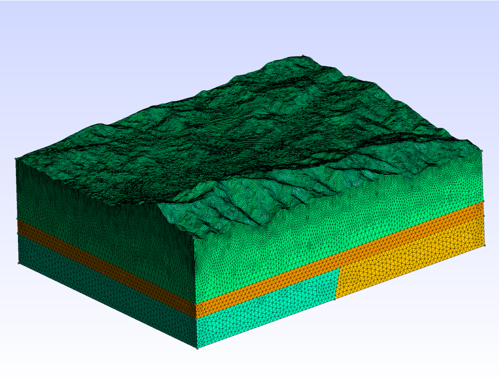

(a) Discretized reservoir model

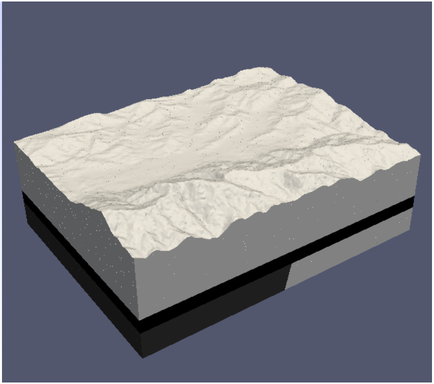

(b) Density model

A model poro-elastic reservoir problem

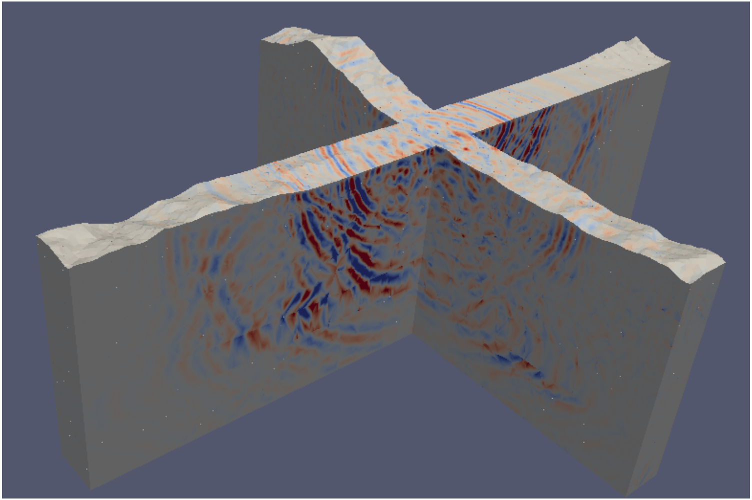

Horizontal fluid particle velocity.

A model poro-elastic reservoir problem

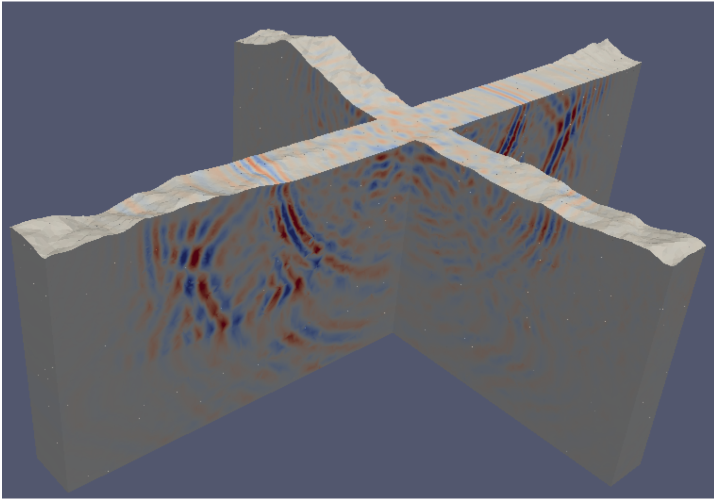

Horizontal solid particle velocity.

A model poro-elastic reservoir problem

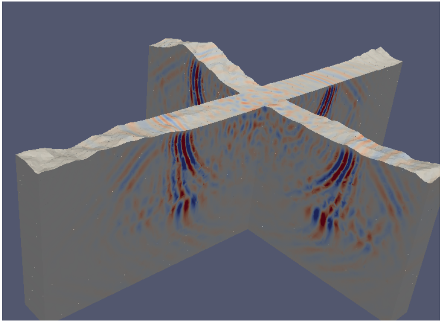

(a) Vertical solid particle velocity

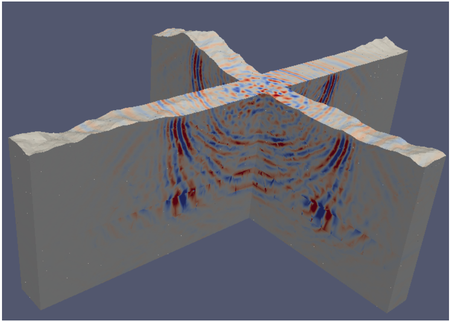

(b) Vertical fluid particle velocity

Extensions and current directions

$$
\begin{bmatrix}
-\frac{1}{2} & q_{12} & q_{13} & q_{14} & & & & & & & & \\
-q_{12} & 0 & q_{23} & q_{24} & & & & & & & & \\
-q_{13} & -q_{23} & 0 & q_{34} & -\frac{1}{12} & & & & & & & \\
-q_{14} & -q_{24} & -q_{34} & 0 & \frac{2}{3} & -\frac{1}{12} & & & & & & \\
 & & \frac{1}{12} & -\frac{2}{3} & 0 & \frac{2}{3} & -\frac{1}{12} & & & & & \\
 & & & \frac{1}{12} & -\frac{2}{3} & 0 & \frac{2}{3} & -\frac{1}{12} & & & & \\
 & & & & \frac{1}{12} & -\frac{2}{3} & 0 & \frac{2}{3} & -\frac{1}{12} & & & \\
 & & & & & \frac{1}{12} & -\frac{2}{3} & 0 & \frac{2}{3} & -\frac{1}{12} & & \\
 & & & & & & \frac{1}{12} & -\frac{2}{3} & 0 & q_{34} & q_{24} & q_{14} \\
 & & & & & & & \frac{1}{12} & -q_{34} & 0 & q_{23} & q_{13} \\
 & & & & & & & & -q_{24} & -q_{23} & 0 & q_{12} \\
 & & & & & & & & -q_{14} & -q_{13} & -q_{12} & \frac{1}{2}
\end{bmatrix}
$$

- Energy stable WADG: immediately extendable to multi-block finite differences through summation-by-parts (SBP) operators.
- Stable WADG for moving curved meshes (r-adaptivity).
- Current: provably stable methods for nonlinear conservation laws.

Kreiss, Scherer (1974). Finite element and finite difference methods for hyperbolic PDEs.

Chan, Hewett, Warburton (2017). Weight-adjusted DG methods: curvilinear meshes.

Guo, Chan (in preparation). Weight-adjusted high order DG methods on moving curved meshes.

Summary and acknowledgements

- Weight-adjusted DG: high order accuracy, provable stability, and efficiency in heterogeneous acoustic-elastic and poro-elastic media.
- This work has been supported by TOTAL E&P Research and Technology USA and the National Science Foundation under DMS-1712639 and DMS-1719818.

Thank you! Questions?

Shukla, Chan, deHoop, Jaiswal (2020). A weight-adjusted DG method for the poroelastic wave equation.

Guo, Chan (2020). Bernstein-Bézier weight-adjusted DG methods for wave propagation in heterogeneous media.

Guo, Acosta, Chan (2019). A weight-adjusted DG method for wave propagation in coupled elastic-acoustic media.

Chan (2018). Weight-adjusted DG methods: matrix-valued weights and elastic wave prop. in heterogeneous media.

Chan, Hewett, Warburton (2017). Weight-adjusted DG methods: wave propagation in heterogeneous media.

Chan, Warburton (2017). GPU-accelerated Bernstein-Bezier discontinuous Galerkin methods for wave propagation.

Additional slides

Existing approaches: mass lumping

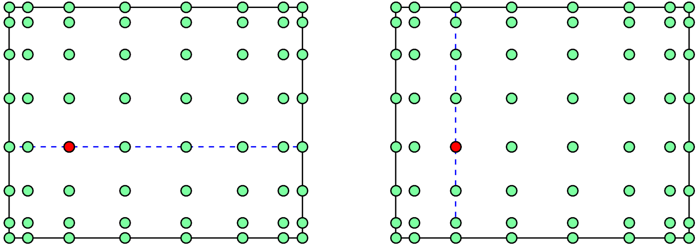

- DG-SEM: collocate at Gauss-Lobatto (or Gauss) points for a diagonal mass matrix. $O(N^4)$ total cost in 3D using Kronecker product.
- Limited to polynomial quads/hexes! Loss of stability or accuracy when extending to simplices (or prisms, pyramids, or non-polynomials).

Chan, Evans (2018). Multi-patch DG-IGA for wave propagation: explicit time-stepping and efficient mass matrix inversion.
Banks, Hagstrom (2016). On Galerkin difference methods.

BBWADG: computational runtime (3D elasticity)

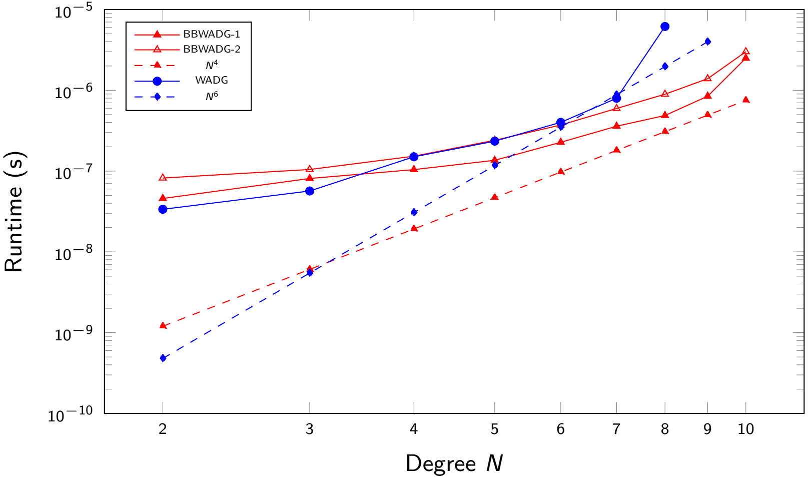

Per-element runtimes of update kernels for BBWADG vs WADG (elastic). For N large, heavy use of register memory results in some loss in performance.

BBWADG: update kernel speedup (3D acoustics)

	$N = 3$	$N = 4$	$N = 5$	$N = 6$	$N = 7$
WADG	1.65e-8	3.35e-8	6.94e-8	1.31e-7	3.28e-7
BBWADG	1.81e-8	2.59e-8	4.22e-8	6.16e-8	9.79e-8
Speedup	0.9116	1.2934	1.6445	2.1266	3.3504

Table: Achieved speedup for $M = 1$

	$N = 3$	$N = 4$	$N = 5$	$N = 6$	$N = 7$
WADG	2.02e-8	4.91e-8	1.20e-7	2.19e-7	4.87e-7
BBWADG	3.60e-8	6.47e-8	9.67e-8	1.51e-7	1.97e-7
Speedup	0.5611	0.7589	1.2409	1.4503	2.4721

Table: Achieved speedup for $M = 2$